PHYSICAL REVIEW VOLUME 74, NUMBER 11 DECEMBER 1, 1948

Studies of Bursts at Sea Level

H. CARMICHAEL
National Research Council of Canada, Chalk River, Ontario, Canada

(Received July 22, 1948)

Data obtained in some 2000 hours of photographic registration of cosmic-ray ionization bursts at sea level (some of which has been published previously) is reported in full. The measurements cover a very wide range of burst size (factor 2000) in two ion chambers of volumes 175 and 1.1 liters, with argon, nitrogen, and hydrogen gas fillings at pressures ranging from 1.5 to 87 atmos. When the ion chambers (thin-walled) are unshielded the bursts are very clearly separable into a component resulting from the extensive cascade showers from the atmosphere and a component resulting from heavily ionizing particles from cosmic-ray induced nuclear disintegrations. The number-size distributions to be expected in the ion chambers from single protons and alpha-particles produced by nuclear disintegrations are calculated on the assumption that these particles have the energy spectrum given by Bagge. The effect of columnar recombination at high pressures in nitrogen and argon is discussed and allowed for. The agreement obtained between the calculated curves and those observed shows that the interpretation of this component as chiefly caused by single heavily ionizing protons and alpha-particles is probably correct. Some very rare bursts of anomalously large size are found under moderate thicknesses of lead. The experimental results of others are reviewed, and detailed comparisons are made.

1. INTRODUCTION

THIS paper is a discussion of a recent remeasurement of old photographic recordings of ionization bursts in two ion chambers of very different size. The recordings were made at sea level, at Cambridge, England, during the years 1935 and 1936 with apparatus that has already been described.[1–3] Only parts[2,4] of the results have so far been published. In the present measurements, bursts of somewhat smaller size have been included because of their probable connection with nuclear fragmentation and the heavily ionizing particles resulting therefrom.

One striking feature of the measurements, which was first noted in 1936[2] and again reported in 1939[4] but which has not so far been fully confirmed by others, is the very steep slope of the size-frequency distribution curve for the smaller bursts (the exponent of the integral curve approaches 6 when the ion chamber is unshielded) followed by a sharp change of slope or *kink* where the readings pass on to the more normal curve of the larger bursts (integral exponent about 1.5). A kinked distribution curve was found both in a large ion chamber at low pressure and in a small ion chamber at high pressure. When first noted in the large ion chamber,[2] the numerous small bursts which produced this change of slope were attributed to the superimposed effects of radioactive alpha-particles statistically coinciding within the resolving time of the apparatus. After a similar change of slope had also been found in an ion chamber at high pressure,[4] the small bursts producing it were thought to be caused by electrons (from the outer fringes of extensive atmospheric showers[5]) because it is known that ionization which is produced by heavily ionizing particles in gases at high pressure tends largely to disappear by columnar recombination. Both these interpretations now appear to be wrong.

Our 1939[4] curves were discussed in some detail by Euler,[6] who calculated the size-frequency distributions to be expected from large cascade air showers[5] originating at the top of the atmosphere and showed that only the less steep parts of our curves could be due to these showers. Euler then postulated that the steeper parts might be connected with the heavy particle stars[7,8] found in photographic plates. He estimated the number of single energetic protons arising from the stars and calculated the distribution curves of bursts that they would be expected to produce at sea level in two cubical ion chambers filled with air at atmospheric

[1] H. Carmichael, Proc. Phys. Soc. **46**, 169 (1934).
[2] H. Carmichael, Proc. Roy. Soc. **A154**, 223 (1936).
[3] Preceding paper by C. N. Chou in this issue.
[4] H. Carmichael and C. N. Chou, Nature **144**, 325 (1939).
[5] Auger, Maze, Ehrenfest, Jr. and Freon, J. de phys. et rad. **10**, 39 (1939).
[6] H. Euler, Zeits. f. Physik **116**, 73 (1940).
[7] E. Schopper, Naturwiss. **25**, 557 (1937).
[8] M. Blau and H. Wambacher, Nature **140**, 585 (1937).

pressure and of volumes 1/4 and 1/100 cubic meters (roughly equal to the volumes of our two ion chambers). For simplicity the cubical ion chambers were supposed to be set at right angles to the paths of the protons. His curves had the required steep slope, and the frequency of bursts was of the right order, but the size of the bursts in the large ion chamber was somewhat too small and in the small ion chamber very much (ten times) too large (see Fig. 8). Euler remarked that the pressure of the gas (82 atmos. argon) in the small ion chamber was not given in our short note to "Nature" [4] and that the calculated size of the bursts would be much reduced if we had used a high pressure.

Following the publication of Euler's paper, Hoffmann,[9] in 1942, reported that he had partly confirmed our experimental curve using a large ion chamber filled with nitrogen at atmospheric pressure. The resolving power for small bursts was enhanced by the use of a multiple electrode system in the ion chamber to shorten the collecting time of the ions. Hoffmann found numerous small bursts which had a very steep

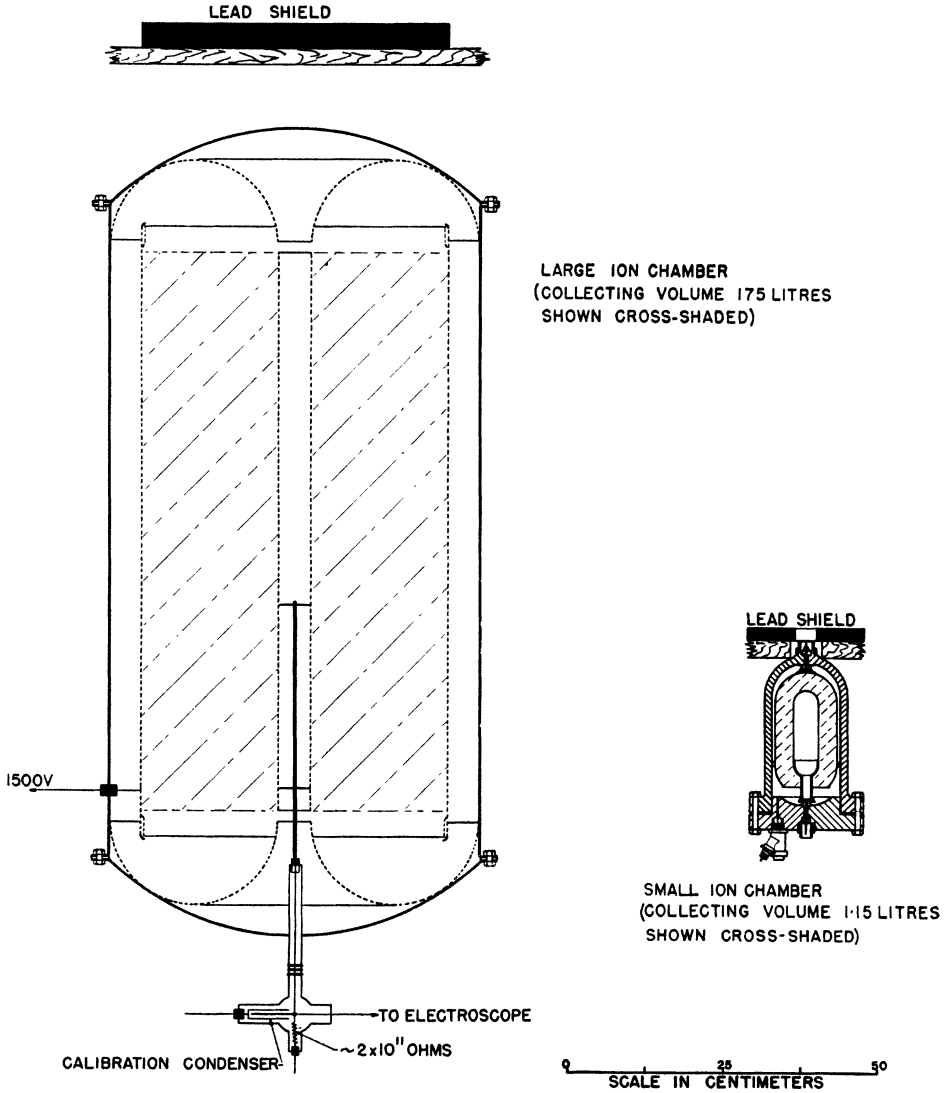

FIG. 1. The two ion chambers and their lead shields.

[9] G. Hoffmann, Zeits. f. Physik **119**, 35 (1942).

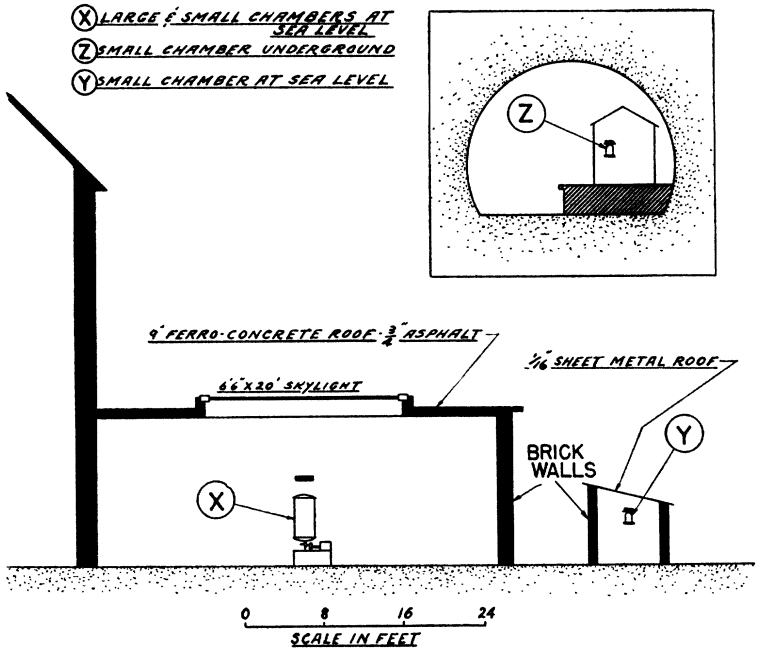

FIG. 2. Details of buildings housing the ion chambers.

distribution curve and, following Euler, he attributed them to protons. His complete curve, however, has a gap at the rather important place where our curve shows a kink because he had to use an alternative, less sensitive, apparatus to record the larger bursts.

Smooth distribution curves, steeper than normal, in unshielded thin-walled ion chambers, have been reported by Street,[10] Montgomery,[11] Schmid,[12] Hoffmann,[9] Clay,[13] and Kingshill and Lewis.[14] Neglecting Euler's argument, Kingshill and Lewis adhered to the view that their bursts were produced by air showers, and they compared their curve with the steeper part of ours on this basis, saying that the less steep branch of our curve must have been produced locally, by mesons, in the walls of the building surrounding our apparatus. When we consider the good agreement obtained by Euler in interpreting this latter part of our curve on the basis of the air showers, it seems that this interpretation of Kingshill and Lewis must be wrong. Their ion chamber and the gas pressure in it were probably too small to show the air showers within the range of frequency which they investigated.

A possible criticism of the experimental work of Kingshill and Lewis is that the range of burst sizes investigated overlaps that of the pulses to be expected in their ion chamber from alpha-particle radioactivity of the walls. However, if the effect of these alpha-particles can be neglected, it can be said that the experimental reality of the steeper part of our curve has now been confirmed both by Hoffmann and by Kingshill and Lewis.

C. G. and D. D. Montgomery more recently[15] have separated out from their sea-level experimental data a steep distribution curve of small bursts which has a rate of occurrence independent of the shielding of the ion chamber. They attribute these bursts to local nuclear processes. In the present paper a slight dependence of these small bursts on shielding is found (see Section 5.2).

The very recent work of Rossi and his collaborators,[16] using powerful new methods of measuring the bursts, has yielded distribution curves which do not have the very steep slope

[10] J. C. Street and R. T. Young, Phys. Rev. **47**, 572 (1935).
[11] C. G. and D. D. Montgomery, Rev. Mod. Phys. **11**, 225 (1939).
[12] H. Schmid. Ann. d. Physik **117**, 452 (1941).
[13] J. Clay and C. G. T. Hooft, Physica **11**, 251 (1945).
[14] K. L. Kingshill and L. G. Lewis, Phys. Rev. **69**, 159 (1946).
[15] C. G. and D. D. Montgomery, Phys. Rev. **72**, 131 (1947).
[16] H. Bridge and B. Rossi, Phys. Rev. **71**, 379 (1947), and papers given at the Washington Meeting in May 1947, Phys. Rev. **71**, 151 (1947).

TABLE I.

Ion-chamber specification	Chamber No.	Gas	Pressure atmos. at 0°C	Shield	Hours	Run No.
Duralumin, volume, 1.15 liters; wall thickness, 1.2 cm	*C*	H_2	6	none	8	*J*
	A	H_2	2.38	none	16	*K*
	A	N_2	60	none	$30\frac{1}{4}$	*L*
	A	N_2	60	Pb disk, 19×2 cm	$7\frac{1}{4}$	*M*
	A	*A*	82	none	$15\frac{1}{2}$	*N*
	A	*A*	82	Pb disk, 19×2 cm	$18\frac{1}{2}$	*O*
	C	*A*	81	none	150	*P*
	B	*A*	87	Pb block, 20×20×1.48 or ×2.05 or ×4.08 cm	119	*Q*
Steel, volume 175 liters; wall thickness, 0.32 cm	*D*	H_2	2.44	Pb disk, 50×4.3 cm	151	*R*
		N_2	1.02	none	98	*S*
		N_2	1.02	Pb disk, 50×4.3 cm	163	*T*
		A	1.52	none	532	*U*
		A	1.52	Pb disk, 50×2.45 or ×4.3 or ×5.8 cm	667	*V*
Wood, volume, 175 liters; wall thickness, 2.5 cm	*E*	Air	Barometric	none	118	*W*

characteristic of those of Kingshill and Lewis, Hoffmann, Montgomery, and the writer; nevertheless this difference is possibly explicable as due to the long cylindrical shape of Rossi's ion chamber (see Section 4.2).

Even in the well established region of the larger bursts, it is surprising how difficult it is to obtain really good quantitative agreement between the results of different experimenters. The kind of agreement that can be obtained has been well shown by Clay[13] but appears good only because the bursts are plotted over a very large range of size and frequency. As will be shown below, our measurements, in the middle part of the curves at least, are probably accurate to within a few percent. If it is assumed that the measurements made by others are equally reliable and that proper allowance has been made for the difference of size of the ion chambers and for the difference of stopping power of the contained gases, the discrepancies which remain can only be ascribed to the influence of the ion-chamber walls and the laboratory surroundings. The surroundings of our apparatus are therefore described in the next section in more detail than previously given.

2. EXPERIMENTAL OBSERVATIONS WITH LARGE LOW PRESSURE AND SMALL HIGH PRESSURE ION CHAMBERS

2.1 Ion Chambers and Surroundings

The two ion chambers are shown to scale in Fig. 1, and also the lead shields and their supporting wooden platforms. A larger drawing of the small ion chamber is given in Fig. 2 of the adjacent paper.[3] It should be noted that the facilities and effort available for these experiments unfortunately did not allow the use of large hemispherical lead shields. The shields used were small and sufficed only to *indicate* the effect of lead.

Details of the buildings surrounding the ion chambers are shown in Fig. 2. For the experiments reported in this paper the apparatus was always at station *X*. Also shown in Fig. 2 (stations *Y* and *Z*) are the sea level and the underground sites used by C. N. Chou, with the same type of apparatus,[2] for the experiments described in the adjacent paper.

Runs were made with various gases in the ion chambers both with and without lead shielding. Particulars of the conditions are given in Table I where the five ion chambers have been distinguished for reference by the letters *A* to *E* and the fourteen different runs by the letters *J* to *W*. It will be noted that in runs *Q* and *V* the results with three different thicknesses of lead have been added together. Runs *P* and *Q* are taken over from the sea-level data obtained by C. N. Chou in station *Y* (reported in the adjacent paper) and supplement the shorter runs *N* and *O* made in station *X*.

2.2 Presentation of the Experimental Results

It has become customary to express the measured size of cosmic-ray bursts in terms of

the number of shower particles per unit area of the ion chamber. This practice involves assumptions about the cause of the bursts (some of which may in fact be caused by heavily ionizing particles) and about the specific ionization of a shower particle in the gas in the ion chamber. It now seems better to revert to the practice of expressing burst sizes in terms of the number of ion pairs collected in the ion chamber, a quantity which is directly measured by the apparatus. This is also in line with the method used by Rossi[16] of standardizing against pulses produced within the ion chamber by alpha-particles from polonium.

In Fig. 3, the integral frequency-size distribution curves obtained in runs J to V of Table I have been plotted in the standard logarithmic manner, the sizes of the bursts being given in

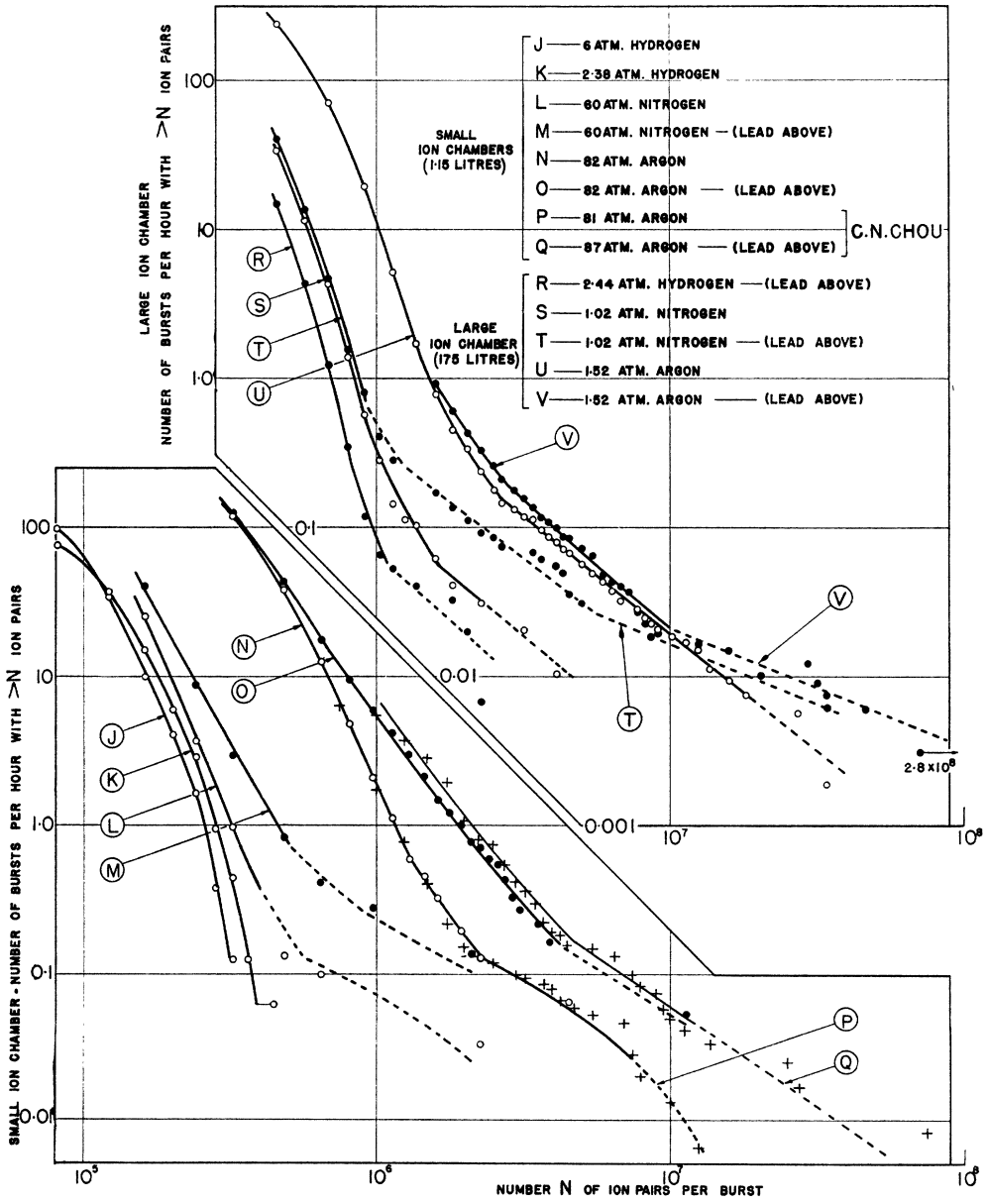

FIG. 3. Integral frequency-size relations.

TABLE II. The experimental data.

Log_{10} Size, 10^6 ion pairs	Log_{10} (No./hr. larger than given size) J	K	L	M	N	O	Log_{10} Size, 10^6 ion pairs	Log_{10} (No./hr. larger than given size) P	Q	Log_{10} Size, 10^6 ion pairs	Log_{10} (No./hr. larger than given size) R	S	T	U	V	W
1.909	1.990	1.925														
0.085	1.528	1.486														
0.210	0.990	1.179	1.397	1.603												
0.307	0.602	0.769														
0.386	0.210	0.449	0.560	0.939												
0.453	$\bar{1}$.573	$\bar{1}$.972														
0.511	$\bar{1}$.096	$\bar{1}$.641	$\bar{1}$.981	0.461	2.074	2.084				0.659	1.168	1.522	1.602	2.379		
0.562	——	$\bar{1}$.097														
										0.756	0.629	1.056	1.131			
0.649		$\bar{2}$.796														
0.687		——	$\bar{1}$.121	$\bar{1}$.918	1.582	1.639	0.875	0.804		0.835	0.083	0.633	0.659	1.844		
0.754										0.902	$\bar{1}$.537	0.133	0.193			
0.812			$\bar{2}$.996	$\bar{1}$.617	1.092	1.241	1.000	0.237	0.741	0.960	$\bar{1}$.075	$\bar{1}$.748	$\bar{1}$.903	1.291		
										1.011	$\bar{2}$.819	$\bar{1}$.447	$\bar{1}$.602			
0.909					0.678	0.973	1.097	$\bar{1}$.891	0.573	1.057	$\bar{2}$.724	$\bar{1}$.155	$\bar{1}$.447	0.710		$\bar{1}$.766
										1.098		$\bar{1}$.051	$\bar{1}$.380			$\bar{1}$.460
0.988				$\bar{1}$.440	0.314	0.762	1.176	$\bar{1}$.609	0.453	1.136	$\bar{2}$.602	$\bar{1}$.001	$\bar{1}$.305	0.230		$\bar{1}$.113
1.055					0.040	0.619	1.243	$\bar{1}$.342	0.294	1.203		$\bar{2}$.788	$\bar{1}$.233	$\bar{1}$.892	$\bar{1}$.965	$\bar{2}$.706
1.113					$\bar{1}$.764	0.473	1.301	$\bar{1}$.185	0.030	1.261	$\bar{2}$.518	$\bar{2}$.612	$\bar{1}$.128	$\bar{1}$.646	$\bar{1}$.782	$\bar{2}$.530
1.164					$\bar{1}$.655	0.314	1.352	$\bar{1}$.124	$\bar{1}$.905	1.312	$\bar{2}$.301		$\bar{1}$.042	$\bar{1}$.526	$\bar{1}$.627	
1.210					$\bar{1}$.508	0.164	1.398	$\bar{1}$.078	$\bar{1}$.875	1.358	$\bar{3}$.826	$\bar{2}$.487	$\bar{2}$.962	$\bar{1}$.374	$\bar{1}$.516	
1.251						0.075	1.439		$\bar{1}$.735	1.399	——		$\bar{2}$.932	$\bar{1}$.247	$\bar{1}$.410	$\bar{2}$.405
1.289					$\bar{1}$.287	$\bar{1}$.988	1.477	$\bar{1}$.000	$\bar{1}$.622	1.437			$\bar{2}$.865	$\bar{1}$.160	$\bar{1}$.321	
1.324				$\bar{1}$.139		$\bar{1}$.879	1.512	$\bar{2}$.969	$\bar{1}$.556	1.472				$\bar{1}$.118	$\bar{1}$.250	
1.356			$\bar{2}$.519	——	$\bar{1}$.110	$\bar{1}$.846	1.544		$\bar{1}$.479	1.504		$\bar{2}$.310		$\bar{1}$.066	$\bar{1}$.192	$\bar{2}$.229
1.386			——			$\bar{1}$.774	1.574	$\bar{2}$.937	$\bar{1}$.354	1.534			$\bar{2}$.827	$\bar{1}$.045	$\bar{1}$.129	
1.414						$\bar{1}$.733	1.602	$\bar{2}$.902	$\bar{1}$.284	1.562			$\bar{2}$.786	$\bar{2}$.981	$\bar{1}$.062	
1.440						$\bar{1}$.636	1.628	$\bar{2}$.823	$\bar{1}$.265	1.588				$\bar{2}$.927	$\bar{1}$.033	$\bar{3}$.928
1.465						$\bar{1}$.511	1.653		$\bar{1}$.201	1.613		$\bar{2}$.009	$\bar{2}$.740	$\bar{2}$.897	$\bar{2}$.988	——
1.489						$\bar{1}$.432	1.677	$\bar{2}$.777		1.637		——	$\bar{2}$.689	$\bar{2}$.853	$\bar{2}$.931	
										1.659			$\bar{2}$.551	$\bar{2}$.830	$\bar{2}$.923	
1.552						$\bar{1}$.335	1.740	$\bar{2}$.727	$\bar{1}$.178	1.700			$\bar{2}$.485	$\bar{2}$.751	$\bar{2}$.856	
1.590						$\bar{1}$.210				1.738				$\bar{2}$.689	$\bar{2}$.809	
							1.813		$\bar{1}$.127	1.773				$\bar{2}$.636	$\bar{2}$.680	
1.657					$\bar{2}$.809		1.845	$\bar{2}$.669	$\bar{1}$.034	1.805				$\bar{2}$.575	$\bar{2}$.638	
					——		1.875	$\bar{2}$.425	$\bar{1}$.002	1.835				$\bar{2}$.504	$\bar{2}$.606	
							1.903	$\bar{2}$.300	$\bar{2}$.923	1.863					$\bar{2}$.573	
										1.889				$\bar{2}$.450	$\bar{2}$.430	
							1.954		$\bar{2}$.877	1.914			$\bar{2}$.389	$\bar{2}$.387	$\bar{2}$.351	
							1.978		$\bar{2}$.767	1.938			$\bar{2}$.263	$\bar{2}$.352		
							2.000	$\bar{2}$.124	$\bar{2}$.701	1.960				$\bar{2}$.315	$\bar{2}$.289	
							2.051		$\bar{2}$.621	2.011				$\bar{2}$.273		
							2.097	$\bar{3}$.814		2.057				$\bar{2}$.228		
							2.138	——	$\bar{2}$.525	2.098				$\bar{2}$.177	$\bar{2}$.217	
										2.136				$\bar{2}$.052		
2.055						$\bar{2}$.733				2.203				$\bar{3}$.973	$\bar{2}$.175	
						——				2.261				$\bar{3}$.876		
										2.312					$\bar{2}$.020	
							2.398		$\bar{2}$.400							
							2.439		$\bar{2}$.224							
										2.437				$\bar{3}$.750		
										2.472			$\bar{2}$.087			
										2.504					$\bar{3}$.953	
										2.534			$\bar{3}$.786	$\bar{3}$.274	$\bar{3}$.874	
										2.668			——	——	$\bar{3}$.778	
							2.875		$\bar{3}$ 922							
							——		——	3.399					$\bar{3}$.483	

ion pairs. The phenomena have been studied over a very wide range of size (factor 2000) with the same recording apparatus, but individual runs do not extend over quite the complete range. The runs with the large ion chamber in Fig. 3 have been vertically separated from those with the small to avoid overlapping of the curves. For convenience of replotting, the logarithmic coordinates of the experimental points are given in Table II.

3. DISCUSSION: LOW PRESSURE DATA, INCLUDING COMPARISONS WITH THE RESULTS OF OTHERS

3.1 General

At their large size ends the curves of Fig. 3 in every case extend out to the largest single burst observed so that near this end they lose statistical accuracy. However, the anomalous slope indicated near the large size ends of curves V and T, obtained with lead shielding above the large ion chamber, is possibly real and may indicate the emergence of a new type of burst found only once or twice per 100 hours at sea level in large low pressure ion chambers. There is also some slight indication (see Section 5.2) of these bursts under lead in the small high pressure ion chamber. They appear to occur only under lead of moderate thickness (2–6 cm) and were not found in unshielded runs or in runs* under large thicknesses of lead. Nor do they appear in the data of the Carnegie meters[17] under 12 cm of lead.

At the small size ends of the curves, the measurements of the recordings have been pushed to the limit at which the bursts disappear within the general fluctuations of the recording. For the last two or three experimental points on each curve, therefore,no great accuracy can be claimed either in the size or the frequency measured, and it would be quite permissible to change the frequencies by a factor of two or more. Because of the logarithmic method of plotting, however, errors of even this magnitude do not much affect the general run of the curves.

In the middle of its range, each of the curves of Fig. 3 is believed on the evidence which follows to be fairly accurate.

The curves N and P, plotted in Fig. 3, were obtained with different ion chambers and different sets of recording apparatus, independently calibrated by different observers (H.C. and C.N.C.). The ion chambers were, however, of the same construction and were filled with argon to about the same pressure (see Table I). The two sets of results coincide very exactly, although the measurements were made in the different stations X and Y of Fig. 2. This indicates that the calibrations of the two sets of apparatus were

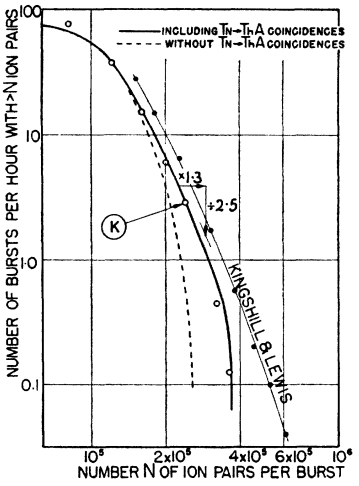

FIG. 4. Comparison of size-frequency distributions, calculated for radioactivity alpha-particles, with experiment.

probably correctly made, and it can also be concluded that the small bursts of the steep branch are not much influenced by the laboratory walls and roof. As regards the larger bursts of the less steep branch, a similar inference cannot be made from this data because run N was not of sufficient duration (see Table I). Actually, work of Montgomery[18] has shown a strong dependence of the larger bursts on the site of his apparatus within the laboratory.

It will be noticed that the corresponding curves O and Q of Fig. 3, taken with lead shielding, do not quite agree. The reason for this is chiefly that the gas in the ion chamber used for curve Q was at rather higher pressure; also the lead shield for curve Q was of rather larger area (see Table I).

A second test of the accuracy of the absolute calibration of the apparatus is obtainable from curves J and K. These are from runs made with two of the small ion chambers filled with hydrogen at the comparatively low pressures of 6 and 2.38 atmos., respectively. At these pressures the mass of gas enclosed is too small to give measurable pulses from cosmic-ray showers. Heavily ionizing particles produced by cosmic radiation would be measurable, but there is no certain evidence of these in the short runs made (a single anomalously large burst occurred in run K). Cosmic-ray effects might be expected to show more strongly in the ion chamber at higher

* Not reported in this paper.

[17] R. E. Lapp, Phys. Rev. **69**, 321 (1946).

[18] C. G. and D. D. Montgomery, Phys. Rev. **56**, 640 (1939).

TABLE III.

Gas	Argon	Nitrogen or air	Hydrogen
Relative stopping power for alpha-particles and protons	1.0	1.0	0.2
Energy spent per ion pair for alpha-particles and protons (ev)	25.4	33.0	35.0
Relative ionization for cascade showers	1.4	1.0	0.2

pressure, whereas the average size of the pulses measured is nearly the same in both ion chambers. Those at the higher pressure actually were smaller by some 6 percent, which is in good agreement with the well-established behavior of alpha-particles, for which columnar recombination of the ions becomes noticeable[19] in commercial hydrogen for the collecting field used here, at a pressure of about 6 atmos. (The crossing over of the curves occurs because alpha-particles were more frequent in one of the ion chambers.) A calculation was made of the distribution curve of pulse sizes to be expected, assuming that the alpha-particles were coming from the natural radioactive elements in the wall material of the ion chamber and that the gas was free from radioactive impurities. The result of this calculation is represented by the full line in Fig. 4, on which the experimental points of run *K* are also shown. The frequency of the calculated pulses is fitted to the experimental frequency at the second experimental point from the left, and the manner in which the rest of the curve matches up with the experimental points provides a very direct confirmation of the calibration of the apparatus. Further details will be given in the next section.

3.2 Influence of Alpha-Particles

As a basis for calculation of the size-frequency distribution of alpha-particle pulses in one of the small ion chambers, it was assumed that the aluminum wall material contained uniform concentrations of both uranium and thorium in equilibrium with their decay products and that the relative amounts were such that the disintegration rates of the two series were equal. It was also assumed that the probability of pulses produced by accidental superposition of two alpha-particles within the resolving time of the apparatus (~0.5 second) was negligibly small. However, there would be additive effects for the relatively rapid (0.1 second) successive thoron and thorium *A* disintegrations from which both of the alpha-particles entered the ion chamber. These were included but not by a rigorously exact method. The calculation was made by S. Kushneriuk of the Chalk River Laboratory using data and formulae given by Evans,[20] and it resulted in the full curve of Fig. 4. The broken curve in Fig. 4 shows the effect of neglecting to add together the coincidences arising from the thoron and thorium *A* disintegrations.

Here, it is of interest to examine the sea-level curve for an argon-filled ion chamber given by Kingshill and Lewis.[14] This curve has been replotted in Fig. 4, where it will be seen that it seriously overlaps the alpha-particle region. Comparison must be made with the calculated alpha-particle curve which includes the thoron, thorium *A* coincidences because the collection time of the ions in Kingshill and Lewis' apparatus was 0.4 sec. In making comparison, the size of the pulses calculated for hydrogen must be increased by a factor 1.3 because less energy is required to produce ion pairs in argon than in argon than in hydrogen (Table III), and their frequency may reasonably be decreased by a factor 2.5 because the walls of Lewis' ion chamber (of four times greater area) were made of steel which usually contains 10 times less radioactive impurity[21] than the aluminum used by the writer. This changes the position of the calculated curve only slightly, as indicated by the arrows in Fig. 4, and so it seems to be very probable that the Kingshill and Lewis data must be considerably affected by alpha-particles unless by some mistake they have underestimated the real size of their bursts (see Section 4.3 in this connection).

3.3 The Kink

The most accurate curve of Fig. 3, (curve *U*) obtained with the large ion chamber unshielded, is replotted in Fig. 5. This curve evidently passes from a steep branch of bursts predominantly of one kind to a less steep branch of bursts pre-

[19] G. Jaffe, Ann. d. Physik **42**, 303 (1913); 1, 977 (1929); Physik. Zeits. **30**, 849 (1929).

[20] R. D. Evans, Phys. Rev. **45**, 29 (1934).

[21] J. A. Bearden, Rev. Sci. Inst. **4**, 271 (1933).

dominantly of another kind. If the two branches are now extrapolated towards each other in the very reasonable manner shown by the broken lines, and if then a combined curve is formed by addition of the two parts, the original curve including the kink is reproduced very exactly. The full line through the experimental points in Fig. 5 is the result of this addition. Assuming with Euler[6] that the smaller bursts with a steep distribution curve arise mainly from nearby nuclear disintegrations, it will now be convenient to call them "fragmentation" bursts and the others, arising from the air showers, cascade[2] bursts.

The kink is therefore associated with the comparative steepness of the distribution curve of the fragmentation bursts as plotted logarithmically. The portion of the composite curve near the kink is given by,

$$N=(23.4)/(P^{1.53})+(1.51\times10^{9})/(P^{7.9}),\quad (15<P<100),\quad (1)$$

where N is the number of bursts per hour which are larger than P and P is the size of a burst in 10^5 ion-pair units.

The distribution curve obtained with the small ion chamber unshielded (curve $(N+P)$ of Fig. 3) has an even more marked kink than the curve U just discussed above, but the analysis of curve $(N+P)$ is more complicated in that it appears to have at least 3 components (see Section 5.2 and Fig. 13). The kink tends to disappear when lead is placed above the ion chamber (curve $(O+Q)$).

3.4 Review of Data on Cascade Bursts in Low Pressure Ion Chambers

In Fig. 5, for comparison with curve U, the sea-level curves given by Bøggild[22] (under a 4.5-cm iron shield), Lapp[17] (1.25-cm iron), and Hoffmann[9] (inside a building) are reproduced as examples of the cascade type of burst and the sea-level curves of Hoffmann,[9] Kingshill and Lewis,[14] and Bridge and Rossi,[16,**] as examples

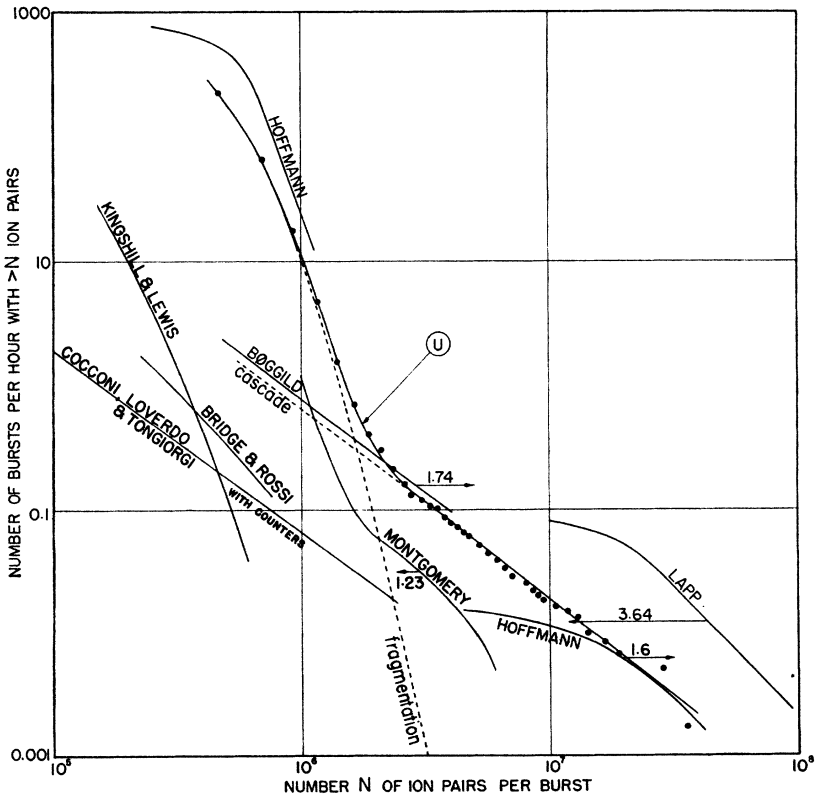

FIG. 5. Analysis of size-frequency distribution in the large ion chamber and comparison with the measurements of others.

[22] J. Bøggild, Die Naturwiss. **23**, 372 (1935).
** Some additional data and an erratum, received privately from Drs. Bridge and Rossi, have been included.

TABLE IV. Experimental conditions for various authors.

Author	C. G. and D. D. Montgomery	Carmichael (curve *U*)	Hoffmann	Boggild	Lapp	Kingshill and Lewis	Bridge and Rossi
Shape of ion chamber	Sphere	Cylinder	Cylinder	Cylinder	Sphere	Sphere	Cylinder
Volume (liters)	50	175	265	35	19.3	22.4	2.3
Diameter (cm)	45	50	?	35	33.3	35	7.6
Length (cm)	——	90	?	60	——	——	51
Gas	Nitrogen	Argon	Nitrogen	Air	Argon	Argon	Argon
Pressure (atmos.)	14.5	1.52	1.0	7	50	1.3	5
Wall material	Magnesium	Iron	Aluminium	Brass with iron ends	Iron	Iron	Brass
Wall thickness (cm)	1.0	0.32	0.15	0.5 brass 1.0 iron	1.25	0.03	0.06(?)
Shielding	Exposed	Building Fig. 2	Building	4.5-cm iron	Exposed	Exposed	Exposed

of the fragmentation type. The curves have been drawn as carefully as possible through the experimental points given by the various authors, without regard for the way in which the authors themselves have drawn their curves.***

The ion chambers are small even compared with the central region of high density of particles expected from the theory[5,23] of cascade showers from the atmosphere. It follows that the frequency of the bursts in two unshielded thin-walled ion chambers of different size will be approximately the same but that the size of the bursts will be proportional to vpq, where v is the volume of the ion chamber, p is the gas pressure, and q is proportional to the stopping power of the gas for the ionizing particles and to the number of ion pairs that are collected per unit energy absorbed. If, on the other hand, the wall of an ion chamber is heavy or if there is heavy shielding material nearby, the size of each burst is liable to be increased by the admixture of narrow showers formed in this shielding by individual high energy electrons of the air showers.

When the above adjustment of size proportional to vpq is applied to the curves of lesser slope in Fig. 5, for comparison with curve U, the resulting changes of size are indicated by the arrows. Good agreement with curve U is obtained only in the case of Lapp. The size of Montgomery's bursts differs by a factor 2.5. The reason for this must be connected with the very light wall material (1 cm magnesium) and good exposure of Montgomery's ion chamber. The disagreement in Bøggild's case is probably explained by the presence of a 4.5-cm iron shield above his ion chamber. The data on which these transformations are based is given in Tables III and IV.

The integral spectrum of extensive showers measured by means of counters at sea level has been given by Cocconi, Loverdo, and Tongiorgi[24] in the form,

$$H(\Delta)=0.124\times10^{-4}/\Delta^{1.46}\ \text{cm}^{-2}\ \text{sec.}^{-1}, \quad (2)$$

where $H(\Delta)$ is the frequency of showers with density $>\Delta$. They have shown that this spectrum is in good agreement with the calculations of Moliere.[23] The integral spectrum of bursts that would be produced by these showers in the ion chamber used for curve U was computed on the assumption that the shower particles produce an ionization in normal argon of 93 ion pairs per cm, corresponding to the minimum value of the energy loss.[25,†] The resulting curve is reproduced in Fig. 5. There is a striking parallelism with Bøggild and with the cascade part of curve U, but the apparent shower densities measured by means of ion chambers are larger than given by counters by the factors: Montgomery, 1.4; Lapp, 3.8; the curve U, 4.3; Hoffmann, 6.3; Bøggild, 9.1. These factors are all too large to

*** In the case of Montgomery (see reference 15), also included in Fig. 5, this procedure has brought to light a detectable bend which looks very similar to the sharp bend in curve U.

[23] G. Molière, Heisenberg's *Cosmic Radiation* (Springer-Verlag, Berlin, 1943), translated by T. H. Johnson (Dover Publications, New York, 1946), Chapter 3.

[24] G. Cocconi, A. Loverdo, and V. Tongiorgi, Phys. Rev. **70**, 841 (1946).

[25] Princeton University data prepared by E. P. Gross (December 1, 1947).

† The writer thanks Dr. J. A. Wheeler for the benefit of a discussion and for forwarding the Princeton data.

be wholly accounted for by cascade multiplication of the showers in the walls of the ion chambers and in nearby dense materials. Evidently the size of the bursts as here computed from the counter data is too small by a factor certainly at least 1.4. This ratio can be accounted for if the average ionization of the shower particles is correspondingly larger than assumed. It is probable that we have here quite a valid experimental indication that high energy electrons have ionization density larger than the minimum, as predicted by Bethe.[26] The cascade electrons of the air showers must have average energy of at least 10^8 ev. A factor 1.4 for cosmic-ray electrons of 10^8 ev is expected theoretically and has been found experimentally by Hayward.[27]

After making this adjustment a ratio of 2.7 still persists between the sizes observed by Lapp and deduced from counters. Cascade multiplication of this amount would not be expected in the 1.25-cm iron wall of Lapp's chamber. Experimental conditions in the other cases are too complicated for comparisons, but there is some experimental evidence which indicates that the $\frac{1}{8}$-inch steel wall of the 175-liter ion chamber used for curve U did not have very much influence on the cascade bursts. This is shown in Fig. 6, where the data of run W of Table II is plotted in comparison with run S. Run W was made with the steel case of the ion chamber replaced by a 1-inch thick air-filled wooden case. The enhancement of the air bursts in site X must therefore have taken place in the thick reinforced concrete roof and brick walls surrounding the apparatus (see Fig. 1). It had been planned also to use this wooden ion chamber out of doors but, unfortunately, this was not done. The record of run W with the wooden ion chamber was, however, much disturbed by "interference," and so is not greatly to be relied upon.

It will be noted that in Bøggild's curve (Fig. 5) there is no trace of fragmentation bursts. However, Bøggild's ion chamber was filled with air at a pressure of 7 atmos., and, therefore, if the fragmentation bursts are caused by heavily ionizing particles, it is possible that they were here suppressed by columnar recombination.[19]

[26] B. Rossi and K. Greisen, Rev. Mod. Phys. **13**, 240 (1941).
[27] E. Hayward, Phys. Rev. **72**, 937 (1947).

The validity of the inference that the fragmentation bursts are in fact produced by heavily ionizing particles (i.e., protons, alpha-particles, or nuclear fragments, of energy less than that for which their specific ionization is a minimum) is strengthened progressively by the experimental evidence from the following sections.

3.5 Comparison of Fragmentation Bursts in Different Gases

Curves R, S, and U of Fig. 3, for the large (175-liter) ion chamber containing hydrogen, nitrogen, and argon, are replotted in Fig. 7. When the size of the bursts of curve U is changed (proportionally to pq, as described in Section 3.4 above) for comparison with curves R and S (see Tables I and III) as shown in broken lines, fairly good agreement is obtained for the cascade bursts only. The fragmentation bursts appear to be too large in nitrogen and much too large in hydrogen.

To explain this discrepancy these small bursts were in 1936[2] ascribed to ionization pulses produced by the chance superposition of several alpha-particles within the resolving time of the apparatus. The writer has, since that time, always been uneasy about this explanation because of the large numbers of natural alpha-particles required and because the small bursts concerned were so sharp and well distinguished from the rest of the recording. It will now be shown, in a preliminary manner, that the spacing and the steep slope characteristic of these curves can be derived on the assumption that they are produced by heavily ionizing particles from nuclear disintegrations.

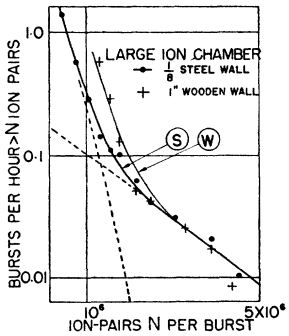

FIG. 6. Effect of replacing the steel wall of the large ion chamber with wood.

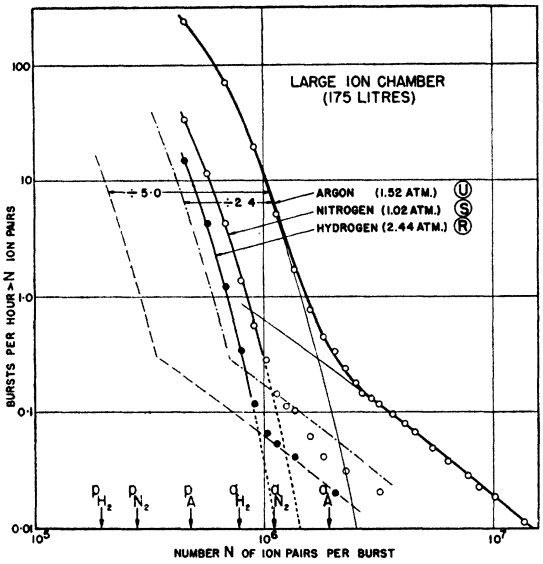

FIG. 7. Comparisons of integral size-frequency distributions in three gases in the large ion chamber.

4. CALCULATIONS OF BURSTS OF IONIZATION FROM HEAVILY IONIZING PARTICLES

4.1 General

The calculation which follows is a modification of the calculation made by Euler.[6] Simple considerations show that the number of bursts produced by disintegrations within the gas in the ionization chamber must be small in comparison with the bursts produced by long range particles from disintegrations in the walls. Euler substituted a cube of side L for the cylindrical ion chamber and considered single protons moving perpendicularly to the face of the cube. He then calculated the number N of bursts of size greater than P.

The observed size of the bursts, i.e., the number of ion pairs produced by the proton in the gas of the chamber, is proportional to the energy P which is lost by the proton in passing through it. If the proton path ends in the gas, $P=E$, where E is the energy with which it enters from the chamber wall, but if the end of the path is lost in the opposite wall, $P<E$. P has a maximum value P_m for a particle which just reaches the opposite wall, because faster particles lose less energy in traversing the gas space. Corresponding to $P<P_m$, there are two possible values of the energy of entrance E: a lower value E_1 for a particle of residual range (R_1) less than L, and an upper value E_2 for a particle of residual range (R_2) greater than L where L is the equivalent air path between the two walls. Therefore, if a proton is observed as a burst larger than P its energy on entering the chamber is between E_1 and E_2. Accordingly, the number N of bursts greater than P is the number of protons for which $E_1<E<E_2$. N can be found from the distribution function $F(E)dE$ which represents the relative numbers of protons in different energy ranges measured in photographic emulsions. For this Euler used the experimental data of Wambacher.[28] The result is shown in Fig. 8 (also containing much other interesting data) taken from Euler's paper.

It is not clear from Euler's paper in what form he used the experimental data of Wambacher. The particles emerging from the wall of an ion chamber have, of course, an energy distribution different from that of the particles as they emerge from stars. The latter is the one given by Wambacher, and the former has been deduced from it by Bagge[29] and given for protons in the form,

$$F(E)dE=(n/4)(A+2BE)(ae^{-E/\epsilon}+be^{-E/\eta})dE, \quad (3)$$

where n is the number of disintegrations per cc (of air equivalent medium) and $A=1.75$, $B=0.88$, $a=3.18$, $b=1.60$, $\epsilon=2.72$ Mev, and $\eta=17$ Mev. Bagge compared this result with a direct measurement of the relative numbers of single proton tracks of different energies made by Widhalm.[30] The two curves are far from similar, and that of Bagge has been chosen for the present calculation because the use of Widhalm's distribution led to unacceptable results on account of the pronounced maximum around 12 Mev.

The function (3) was integrated (with $n=1$) to obtain the number of protons as a function of energy in the form,

$$N=\int_E^\infty F(E)dE, \quad (4)$$

where N is the number having energy $>E$. Representative values of N are given in Table V.

Let us now consider the maximum sizes of bursts that single protons could produce in the

[28] H. Wambacher, Physik. Zeits. **39**, 887 (1938).
[29] E. Bagge, Ann. d. Physik **39**, 512 (1941).
[30] A. Widhalm, Zeits. f. Physik **115**, 481 (1940).

ion chamber. Such protons would travel along the longest path in the collecting space and come to the end of their range just as they reached the other side. These maxima for the three gas fillings are shown by arrows in Fig. 7, and it is seen that they are too small, by a factor of more than 4, to account for the largest fragmentation bursts. The corresponding maxima for alpha-particles are also shown. They are slightly too small. It may therefore be assumed that the largest fragmentation bursts are produced by single alpha-particles accompanied by one or two protons, or that rather large numbers of simultaneous protons are involved. The steep slope of the curves makes the alpha-particle hypothesis the more attractive one. A calculation for alpha-particles follows in the next section, and so as to make the work more complete calculations are also made for the ion chambers used by Bridge and Rossi[16] and by Kingshill and Lewis.[14]

4.2 Calculation of Bursts Caused by Single Particles from Stars††

As no experimental data on the energy spectrum of alpha-particles in stars has been published, we make the assumption that it is the same as that observed for protons. Then the numbers of Table V apply also to alpha-particles, except that the absolute values are smaller because the ranges are shorter and because fewer are presumably emitted per disintegration.

The range-energy relation for alpha-particles is approximated in the form

$$R=kE^n, \quad (R(\text{cm}); \quad E(\text{Mev})), \tag{5}$$

where $k=0.15$ and $n=1.8$.

If L is the equivalent air path between the walls of the ion chamber, the two particle energies, E_1 and E_2, which give the same pulse size P as described above, are given by

$$E_1=P=(R_1^{1/n})/(k^{1/n}) = (R_2^{1/n}-(R_2-L)^{1/n})/(k^{1/n}) \tag{6}$$

and

$$E_2=(R_2^{1/n})/(k^{1/n}). \tag{7}$$

Hence the number N of particles with energy between E_1 and E_2, which is the number giving bursts of size greater than P, was obtained (from a plot of Table V) as a function of P for a given

TABLE V. Integral energy distribution of single protons in photographic emulsion according to Bagge.

E Mev	$\int_E^\infty F(E)dE$ for 1 disintegration per cc
150	0.3
100	3.9
90	6.5
80	10.7
70	17.2
60	27.5
50	42.8
40	66.0
30	98.6
20	140.3
15	163.5
10	187.0
5	210.3
0	229.4

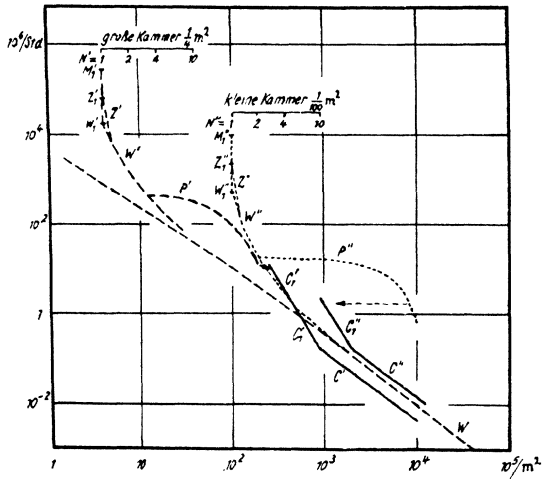

FIG. 8. H. Euler, see reference 6. (Reproduced from Zeitschrift fur Physik.) "Distribution of bursts in unshielded ion chambers. Abscissa: density of rays per m² (number N of electrons which simultaneously strike the chamber, divided by the horizontal cross-sectional area). Ordinate: frequency of bursts per hour whose density is greater than that given by the abscissa. $WW'W''$: bursts by air showers of the primary electrons (theoretical). $P'P''$: bursts caused by individual protons, whose ionization exceeds that of the number of electrons given by the abscissa (deduced for chambers with normal pressure, from Wambacher's measurements). ('): for a large chamber of ¼ sq.m of cross-sectional area. (''): for a small chamber of 1/100 sq.m of cross-sectional area. $C'C_1'$: measurement by Carmichael with a 175-liter chamber. $C''C_1''$: measurement by Carmichael and Chou with a 1-liter chamber. (For the extrapolation to a chamber with a zero ion-collection time: $M_1'M_1''$: ionization bursts of individual mesons. $Z'Z''$: small bursts by air showers of the electrons that have arisen fron the decay of mesons in the lower atmosphere.)" (Translated from the German—see reference 6.)

†† The writer thanks V. H. Rumsey of the Theoretical Branch of the Chalk River Laboratory, now at the Ohio State University, for generous help in setting up these calculations.

TABLE VI. Integral distribution of paths in three ion chambers with total numbers equal to the wall areas in sq. cm.

Ion chamber D, path length cm	Integral number of paths	Kingshill and Lewis, path length cm	Integral number of paths	Bridge and Rossi, path length cm	Integral number of paths
100.0	0	35.2	0	51.0	0
95.0	100	34.9	100	45.0	1
91.0	300	34.2	300	31.0	3
84.0	500	33.5	500	27.0	5
78.0	700	32.7	700	24.8	7
73.0	900	31.9	900	23.2	9
67.0	1250	30.4	1250	21.2	12.5
61.8	1750	27.9	1750	19.4	17.5
57.0	2500	23.4	2500	17.5	25
53.1	3500	15.5	3500	15.9	35
50.8	4500	0.0	3850	14.8	45
49.4	5500			13.9	55
47.7	6500			13.2	65
45.6	7500			12.7	75
43.0	8500			12.2	85
40.0	9500			11.8	95
36.7	10500			8.3	300
33.0	11500			7.7	500
29.1	12500			7.1	700
25.0	13500			5.8	900
20.7	14500			2.5	1250
16.2	15500			0.0	1304
11.4	16500				
6.3	17500				
0.0	18060				

value of L. This was done for several values of L throughout the complete range of the air equivalent path L found in the various ion chambers. Since at this stage we are not interested in absolute values but only in the shape of these curves for different L, all the curves were now scaled to a total ($N_0 = \int_0^\infty F(E)dE$) of 100 particles of all energies, and P was expressed as a percentage of its maximum value for each value of L. The curves for different L are very similar in shape, a fact which partly accounts for the parallelism of the steep parts of the curves R, S, and U of Fig. 7. Three of the curves are reproduced in Fig. 9 (for $L = 20$, 50, and 150 cm). They correspond to the proton curves for values of L about 10 times as large (as found in the small ion chamber, see Section 5.4).

So far we have been concerned with the number N of bursts of size greater than P produced in an air gap of thickness L by a total number N_0 of particles having energy distribution $F(E)dE$ emerging perpendicularly from one wall of the air gap. We now take account of the actual geometrical shapes of the various ion chambers, considering them to be irradiated by particles which emerge in all directions from the wall. The wall will be assumed to be thick compared with the ranges of the particles.

It is evident, because the nuclear disintegrations are distributed uniformly throughout the material of the wall, that the energy distribution of the emerging particles will be independent of the angle with the normal to the wall at which they emerge, and that the number emerging from given area into a small solid angle in any particular direction making angle θ with the normal will be proportional to $\cos\theta$ (Knudsen's law).

We may regard, therefore, the inner surface of the ion-chamber wall as a uniformly distributed source such that the density of paths per unit solid angle per unit area of wall in any particular direction is to be proportional to the cosine of the angle with the normal to the surface from which the paths originate. We are required to know the total number of such paths inside the ion chamber, with lengths between L and $L+dL$. Though this problem is easy for a sphere, it appears tedious for a short cylinder. A simple mechanical apparatus was therefore constructed which enabled the required distribution to be obtained very rapidly by direct measurement, using scale models of the various ion chambers.

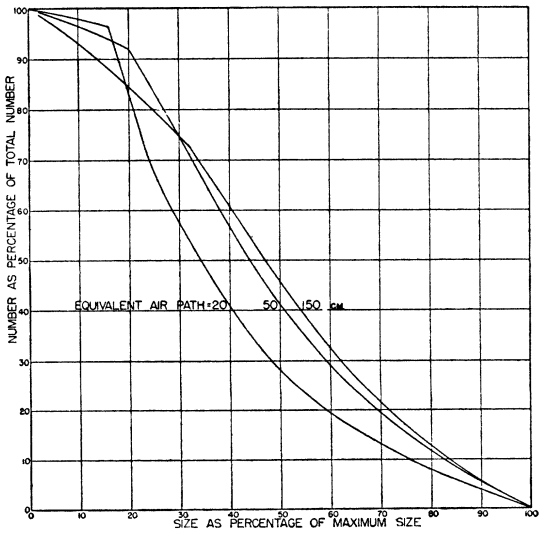

FIG. 9. Calculated bursts, caused by alpha-particles with a Bagge energy distribution directed normal to the walls of a parallel plate ion chamber.

The number of paths of length greater than L in the ion chambers of Bridge and Rossi, Kingshill and Lewis, and the writer, assuming in each case the total number of paths to be equal to the wall area of the ion chamber in square centimeters, is given in Table VI.

The equivalent air path L' for each gas and pressure was next found by the relation $L'=psL$, where p is the pressure in atmos. and s is the stopping power of the gas relative to air (see Tables I, III and IV) and substituted for the path lengths in Table VI.

Now for each value of L' the energy P_m of an alpha-particle of that range was substituted. Then, by means of Fig. 9, the number δN of paths appropriate to each value of P_m was replaced by an equal number of bursts with a distribution in size suitable for the corresponding value of L'. Finally the size of P of the bursts was converted into the number of ion pairs appropriate for the various gases (Table III). The resulting five curves for the bursts from single alpha-particles, plotted on logarithmic scales, are given in Fig. 10. The curves for the bursts caused by single protons are of approximately the same shape as these, with the size of the bursts reduced by a factor four. It may be noted that the curve calculated for the long cylindrical ion chamber of Bridge and Rossi is not so steep as the other curves. Their measurements (see Fig. 5) show a similar characteristic.

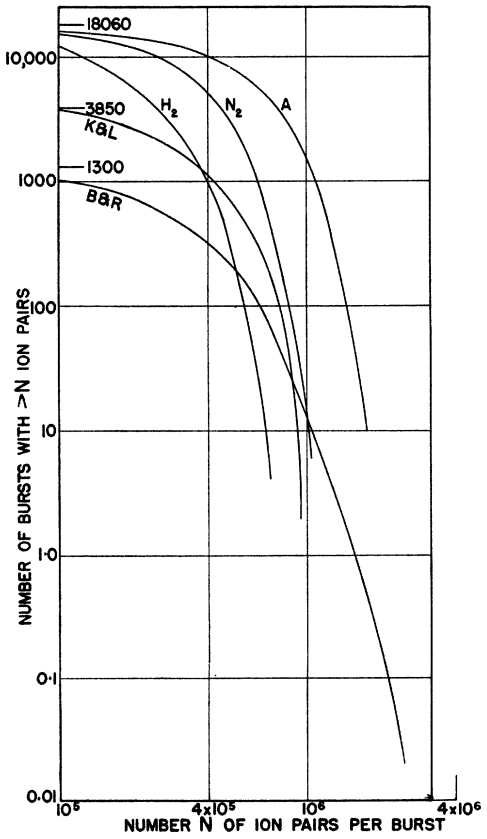

FIG. 10. Calculated bursts in various ion chambers caused by cosmic-ray induced alpha-particles.

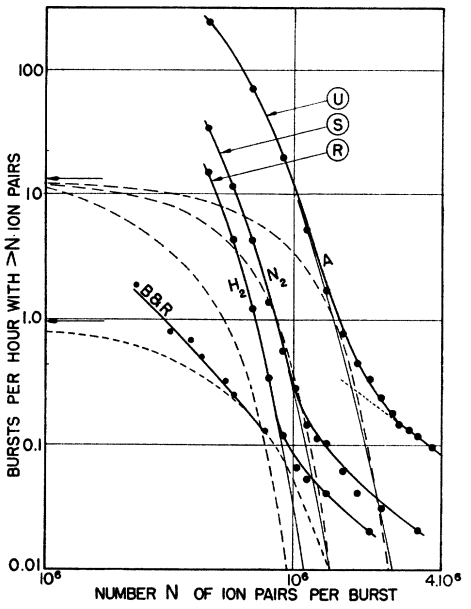

FIG. 11. Comparison of calculated alpha-particle bursts with experiment.

4.3 Comparison with Experiment

In Fig. 11 the calculated curves of Fig. 10 are shown fitted *both* as regards frequency and size to the steep parts of the experimental curves R, S, and U and to the experimental curve of Bridge and Rossi (i.e., the relative positions of the calculated curves have not been changed). It does not seem to be possible to obtain at the same time agreement with the measurements of Kingshill and Lewis. With the superposition used in Fig. 11 the bursts calculated for the Kingshill and Lewis ion chamber are almost exactly twice as large as those observed. If, in fact, Kingshill and Lewis have underestimated the real size of their bursts, the uncertainties about possible confusion with natural alpha-particles, already discussed above, would disappear; but it must

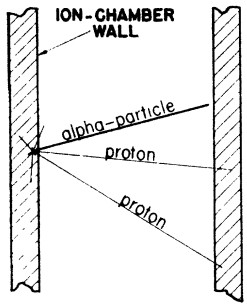

FIG. 12. Showing how the alpha-particle bursts are probably on the average somewhat increased in size by one or two long range protons coming from the same disintegration.

also be noted that their ion chamber had an extremely thin wall (see Table IV).

With the superposition shown in Fig. 11, the rate of occurrence of bursts is determined chiefly by the curve of Bridge and Rossi, but it is noteworthy that this brings the end point of the calculated curve U directly beneath the kink in the experimental curve. There is ideally a small step at the kink corresponding to the length of the cylindrical ion chamber. In other ion chamber configurations (e.g., a sphere) such discontinuities might be much more pronounced.

The calculated curves fit the experimental curves S and U for argon and nitrogen remarkably well as regards their relative spacing and their slope. There is a 10 percent discrepancy of relative size in the case of the hydrogen curve R.

The fact that the observed bursts in hydrogen are not smaller in size than is calculated in this way is evidence that few of these bursts appear to originate directly from nuclear disintegrations in the gas in the ion chamber (because no disintegrations would occur in hydrogen). Some part of the 10 percent excessive size observed in hydrogen can be attributed to the heavier gases usually present as impurities in commercial hydrogen. Another part should be attributed to proton recoils produced by the fast neutrons of the nuclear disintegrations, but this is estimated to be rather small. However, there is some (rather unreliable) experimental evidence in Fig. 6 that a similar discrepancy exists when the ion chamber has a wooden (hydrogenous) wall.

To obtain the fit shown in Fig. 11 it was necessary to increase the size of all the calculated bursts by a factor 1.40 which would appear to be well above experimental error. It is possible that particles of larger mass or charge than alpha-particles are involved, but it seems to be more probable that this discrepancy is due to the protons which must be expected to accompany these single alpha-particles. The protons from a nuclear disintegration may be more numerous and of longer range (by a factor 10) than the alpha-particles, and so it is probable that many of the alpha-particles crossing the ion chamber are accompanied by two or more protons which may increase the observed ionization bursts by about 40 percent. An illustration of what is meant is given in Fig. 12. Thus the curves calculated for alpha-particles, as fitted to the experimental curves in Fig. 11, represent the number of those alpha-particles in the ion chamber which are accompanied by about this amount of proton ionization and do not necessarily represent all the alpha-particles which may be entering the ion chamber from nuclear disintegrations. With this reservation we can deduce, by comparison of the vertical scales of Figs. 10 and 11, that the number of these alpha-particles emerging from an iron surface at sea level is

$$N_0 = 1.77 \times 10^{-2} \text{ per sq. cm. per day.}$$

As a result of introducing the actual geometrical shape of the ion chamber, these calculations have provided a somewhat longer steep slope than was obtained by Euler, but they then depart from the experimental curves rather suddenly. It may be that the distribution function, Eq. (3), as Bagge has already suggested, should have included very many more short-range particles. Some allowance also may be made for inaccuracy of the experimental observations in that a large number of spurious fluctuations have probably been included as bursts in this region. The remainder of these smaller bursts may possibly be ascribed to groups of protons, but there seems to be definite discrepancies here with the observations made with the small ion chamber now to be discussed.

5. DISCUSSION: HIGH PRESSURE DATA

5.1 General

As already mentioned above, there is a possibility of distinguishing between heavily ionizing and thinly ionizing particles in ion chambers at

high pressures because columnar recombination depends upon the gas, the pressure, and the line density of the ionization. The measurements made with the small ion chamber in argon at 82 atmos. (curves $(N+P)$ and $(O+Q)$) and in nitrogen at 60 atmos. (curves L and M, Fig. 3) are convenient for a preliminary study of these effects. The discussion in Section 5.3 will show that in argon columnar recombination is negligibly small with the field strength used (460 v/cm), even at 82 atmos., for the thinly ionizing electrons of the cascade showers. This fact will be used in the following section for making an empirical analysis of the argon curves into separate components.

5.2 Analysis of Distribution Curves

Referring to curve $(N+P)$ in Fig. 13, for the unshielded ion chamber, evidently there is a very steep component which has provisionally been labeled "protons, unshielded." With the small chamber there was no anxiety over the reality of these small bursts because they were very clearly distinguishable from fluctuations of the background.

It is reasonable to include next a component representing the large air cascades, and this was taken over directly from the measurements made in the same site with argon in the large ion chamber. The size of the bursts was changed, as already described in Section 3.4, and recombination was assumed to be negligible. This component is labeled "cascade, unshielded."

There is now room for a third component, very similar in shape to the curves calculated above for alpha-particles, provisionally labeled "fragmentation alphas." By addition of these three components the curve $(N+P)$ is reproduced as shown by the full line through the experimental points.

Referring now to curve $(O+Q)$ in Fig. 13, obtained with about 2 cm of lead above the ion chamber, it is reasonable first to increase the size of the cascade bursts by a factor appropriate for this thickness of lead. Best fit is found using a factor 3, which does not seem to be unreasonable. Montgomery found, experimentally, 1.88 for 1 cm of lead.[15] This component is labeled "cascade, lead."

It seems not to be possible to reproduce the curve measured under lead without also making, as shown, a substantial change to the steep curve labeled "protons, unshielded." The curve marked "protons, lead" was substituted. The experimental accuracy is not sufficient to decide if a change should also be made in the "fragmentation alphas" under lead.

An anomalous slope for the largest bursts under lead very similar to that found with the large ion chamber is indicated.

It appears that no data has been published which can be used to corroborate the analysis just given. Before further discussion of these bursts in high pressure gases, it will be necessary to discuss columnar recombination.

5.3 Columnar Recombination

A good historical summary with references, of the attempts that have been made to develop a theory of recombination in gases at high pressures, has been given by Broxon and Meredith.[31]

The theory of columnar recombination derived by Jaffe in 1913[19] is generally accepted as fairly reliable for the alpha-particles from radioactive substances, in gases such as air, carbon dioxide, etc., within a moderate range of pressures, up to about 10 atmos., in which measurements have been made. The theory uses the average value

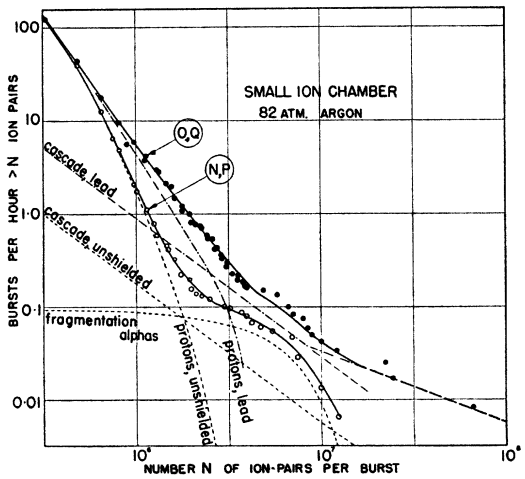

FIG. 13. Analysis of size-frequency distributions in the small ion chamber.

[31] J. W. Broxon and G. T. Meredith, Phys. Rev. **54**, 9 (1938). (It is important to study this paper in conjunction with a correction made on page 605 of the same volume of Phys. Rev.)

of the mobilities of the positive and negative ions, and so its application to gases such as pure argon, where it is known that most of the negative ions are electrons with mobility of the order 1000 times that of the positive ions, is probably unjustified. This has been pointed out by Klema and Barschall.[32] Difficulties also appear with more thinly ionizing particles and electrons. The theory has been applied to gamma-ray ionization up to pressures of the order of 100 atmos. by Clay,[33] Lea,[34] Broxon,[31] and others. This led to a controversy between Clay[35] and Lea[36] over the merits of a rival "cluster" theory, developed by the latter for ionization produced by gamma-radiation. Here we shall make only formal use of the Jaffe theory to calculate short extrapolations of experimental data for nitrogen and for argon.

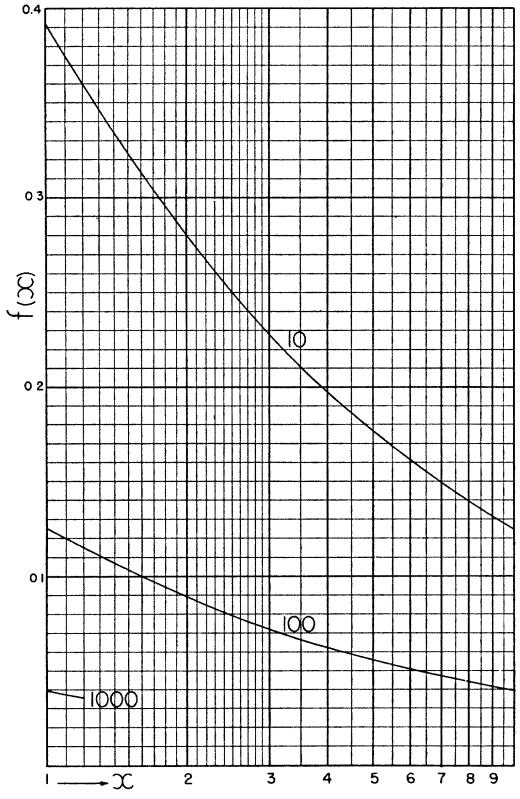

FIG. 14. Extension of the Zanstra curve (see reference 37) from $x=10$ to $x=1000$. Thus for $x=160$, $f(x)=0.1$

The Jaffe formula can be written,

$$1/c=1+qf(x), \tag{8}$$

where c is the fraction of the ions in the column which escapes recombination and is collected.

The function $f(x)$ has been given graphically by Zanstra[37] for values of x from 10^{-8} to 12. This range of values has been extended††† in Fig. 14 to $x=1000$ to cover our needs in this paper.

The variables q and x are functions of the following: N_0 = the initial line density of ions in a column, α = the recombination coefficient of the ions, D = the diffusion coefficient of the ions, u = the mobility of the ions, assumed the same for both kinds, ϕ = the angle between the column axis and the collecting field, E = the intensity of the collecting field, and b = a parameter proportional to the initial "radius" of the cylindrical column. We may assume that N_0, α, D, u, and b are either proportional or inversely proportional to the pressure p in the range over which we wish to extrapolate. Then,

$$q=(\alpha'/8\pi D')N_0'p \tag{9}$$

and

$$x=(b'/p)^2(u'/2D')^2E^2\sin^2\phi, \tag{10}$$

where α', etc., are the appropriate (but not necessarily the actual) values at a pressure of one atmos.

Numerical values for the constants α', D', and u' may now be inserted. However, α' and D' are both proportional to u' as follows:

$$\alpha'=8\pi eu=8\times3.14\times4.8\times10^{-10}\times300\mu' =3.6\times10^{-6}u'^{38}$$

and

$$D'=0.0236u' \text{ (for } u' \text{ in cm/sec./volt/cm)}.^{39}$$

These relations can be checked by means of the value of $\alpha'p$ measured by Lea[34] in an ion chamber filled with nitrogen. Lea found $\alpha'p=5.7\times10^{-6}$ in the pressure range 20 to 90 atmos. Hence, $u'=5.7/3.6=1.6$ sec.$^{-1}$ volt^{-1}, which is close to the accepted value for nitrogen, and $D'=0.0236\times1.6=0.038$, instead of the 0.035 usually quoted.

[32] E. D. Klema and H. H. Barschall, Phys. Rev. **63**, 18 (1943).
[33] J. Clay, Phys. Rev. **52**, 143 (1937).
[34] D. E. Lea, Proc. Camb. Phil. Soc. **30**, 80 (1940).
[35] J. Clay and M. Kwieser, Physica **7**, 721 (1940).
[36] E. Kara-Michailova and D. E. Lea, Proc. Camb. Phil. Soc. **36**, 101 (1940).
[37] H. Zanstra, Physica **2**, 817 (1935).
††† By the Theoretical Branch of the N.R.C. Chalk River Laboratory.
[38] J. D. Cobine, *Gaseous Conductors* (McGraw-Hill Book Company, Inc., New York, 1941), p. 100.
[39] L. B. Loeb, *Kinetic Theory of Gases* (McGraw-Hill Book Company, Inc., New York, 1934), p. 555.

Equations (9) and (10), therefore, become

$$q = 6.1 \times 10^{-6} N_0' p \qquad (11)$$

and

$$x = 2.24 \times 10^2 (b'/p) E^2 \sin^2\phi \qquad (12)$$

for p in atmos. and E in volts per cm. The arbitrary parameter b' remains to be adjusted; b' should be dependent only on the nature of the gas.

No measurements of recombination appear to have been made with heavily ionizing particles at the high pressures used in the small ion chamber. Commercial nitrogen, however, has recently been carefully studied up to 41 atmos. by Dick, Falk-Variant, and Rossel.[40] They offer no data for argon. For argon we can use some unpublished data at 20 atmos. obtained in this laboratory by Craig[41] with commercial oxygen-free argon similar to that with which the small ion chambers were filled. Craig also studied commercial nitrogen at 20 atmos.

From Dick, Falk-Variant, and Rossel the fraction of the total number of ion pairs produced by ThC alpha-particles, collected by a field of 7550 volts per cm at 41 atmos. in nitrogen, was 0.32. Using the averages $\sin^2\phi = 0.5$ and $N_0' = 3.7 \times 10^4$ in Eqs. (8), (11), and (12), we find $b' = 1.9 \times 10^{-3}$ cm. The nitrogen data of Craig at 20 atmos., for the short-range alpha- and lithium particles of the boron disintegration, leads to a slightly higher value of b'. We therefore take $b' = 2.0 \times 10^{-3}$ cm for commercial nitrogen (containing 0.5 to 1.0 percent of oxygen).

In argon, with 200 volts per cm, Craig found, for the boron disintegration particles, 72 percent collection at 20 atmos. Hence ($N_0' = 8.7 \times 10^4$) $b' = 0.2$ cm for commercial oxygen-free argon.

With these values of b' the calculated percentages of ions collected in the small ion chamber (field 460 volts per cm), for both protons and alpha-particles in nitrogen and argon at various energies between the end of the range and minimum ionization, are given in Table VII. It can be seen that the amount of recombination found for argon is almost negligible except for alpha-particles of comparatively low energy, and so use of the exceptionally large value of b' in argon, which was called for by the Jaffe theory, need cause no misgivings.

[40] L. Dick, P. Falk-Variant, and J. Rossel, Helv. Phys. Acta 22, 357, 362 (1947).

[41] D. S. Craig (1947) N.R.C. Chalk River Laboratory, unpublished.

TABLE VII. Fractions C of ions collected in the small ion chamber in nitrogen and argon for protons and alpha-particles of specified energies.

Energy Mev	N_0 in standard air		C in nitrogen 61 atmos.		C in argon, 82 atmos.	
	proton	alpha	proton	alpha	proton	alpha
0.5	1.40×10^4	5.6×10^4	0.054	0.015	0.68	0.35
1.5	6.16×10^3	2.46	0.12	0.027	0.83	0.55
3	3.85	1.54	0.18	0.05	0.88	0.66
6	2.25	9.0×10^3	0.27	0.08	0.93	0.77
10	1.47	5.9	0.36	0.12	0.95	0.84
30	6.17×10^2	2.47	0.57	0.25	0.98	0.92
70	3.19	1.27	0.72	0.39	0.99	0.96
200	1.48	5.9×10^2	0.84	0.58	1.00	0.98
600	8.43×10^2	3.37	0.91	0.71	1.00	0.99
1000	7.31	2.92	0.92	0.74	1.00	0.99

5.4 Comparison in Two Gases at High Pressure

Equipped with the data of Table VII it is possible to predict the sizes of the ionization bursts to be expected for both the argon and nitrogen fillings for any kind of ionizing particles. Hence number-size relations can be calculated for single mesons, protons, or alpha-particles by the method of Section 4.

(a) *Mesons*

Although the pulses produced by single high energy mesons are not observable in the small ion chamber, it is of interest to calculate their distribution curves for the nitrogen and the argon fillings. A calculation was based on the approximate distribution of straight paths given in Table VIII. This was derived from the distribution measured for the large ion chamber, Table VI, making an allowance for the obstruction of the large central electrode of the small ion chamber. It was assumed that each meson produced a uniform line density of ion pairs corresponding to an energy loss of 1.825 Mev per g per cm[2,25] in air (68 ion pairs/cm in air) and that the flux of mesons at sea level (including also the single electrons) was 1.0 per sq. cm. per minute. The ion chamber was considered to have an effective horizontal area of 120 sq. cm. Collection of the ions was taken to be 100 percent in argon and 92 percent in nitrogen (Table VII). The resulting curves, which correspond to the single point M_1'', of Euler in Fig. 8 are shown in the top left-hand corner of Fig. 15.

TABLE VIII. Integral distribution of paths in the small ion chamber with total number equal to the wall area in sq. cm.

Integral number of paths	Path length, cm
5	20
25	18
125	13
325	10
825	5

The distribution curves for single mesons and electrons as plotted in Fig. 15 are strongly curved. Inclusion of the larger pulses to be expected from more heavily ionizing electrons of high energy and from slow mesons will tend to swing the lower ends to the right. However, from the data of Sands[42] it appears that only about 10 mesons per hour will stop in the chamber, and so the bursts from single slow mesons, although some are of measurable size, are unimportant in comparison with the number of small bursts observed.

(*b*) *Protons*

The small ion chamber with argon has a maximum path equivalent to about 1600 cm of air, or 2.0 g/cm^2. A proton of this range has energy 44 Mev and so, assuming recombination negligible (Table VII), will produce a burst of 1.7×10^6 ion pairs. This burst size is marked $P_{\max}{}^A$ in Fig. 15.

For the nitrogen filling the maximum path in the ion chamber is equivalent to about 1200 cm of air. To find the number of ion pairs collected in the ion chamber for a proton of this range, an "ion-pairs—range" relation (analogous to the energy—range relation) was deduced by graphical integration from the data of Table VII. In this the number of ion pairs was the total that would be collected over the range after allowing for columnar recombination. Hence the burst size for a 1200-cm proton with the nitrogen filling is 4.8×10^5 ion pairs. This is marked $P_{\max}{}^{N_2}$ in Fig. 15.

The maximum proton burst in argon is 3.5 times as large as the maximum proton burst in nitrogen, and this ratio is the same as that of the observed bursts of the steep branches and is 1.75 times that calculated for thinly ionizing particles. The absolute sizes also are in fair agreement. These steep branches of small bursts in the small ion chambers are therefore provisionally identified as produced mainly by single protons.

It is now desirable to assume an energy distribution or spectrum for these protons and from it calculate the distribution of burst sizes for both the argon and nitrogen fillings for a more thorough comparison with experiment. This was first done on the assumption that the protons had the Bagge energy distribution (Eq. (3)). The distribution of paths in the ion chamber given in Table VIII was used. In argon, where recombination could be neglected, the calculation was very similar to that already outlined in Section 4.2. In nitrogen, where bursts produced by protons stopping in the ion chamber have recombination different from bursts of the same size produced by protons passing out of the ion chamber, the calculation was more complicated and only an approximate result was obtained. The resulting curves, fitted as regards frequency to the observed curves, are labeled "Bagge protons" in Fig. 15. The relative spacing of the calculated curves fits that of the observed curves very well, and the slope is moderately well represented for the larger bursts. The number of protons of all ranges (in isotropic Bagge distribution) from an aluminum surface at sea level, corresponding to the fit of the calculated curves of Fig. 15, is

0.67 per sq. cm per day.

The calculation conspicuously fails to provide a sufficient number of small bursts. The deviation is sudden and very similar to that already found for alpha-particles in the large ion chamber. It should be noted again here that Bagge himself has stated, on the basis of a comparison with the photographic data of Widhalm, that protons of short range appear to be more numerous than given by Eq. (3).

Larger numbers of small bursts can be obtained from protons in another way. It has been stated[43] that most of the "positive excess" of high energy cosmic-ray particles may consist of protons. To see what the distributions of bursts from such protons would look like, we may assume that the distribution function $F(R)$ of

[42] M. Sands, Washington Meeting (1948), Section 8.

[43] Adams, Anderson, Lloyd, Rau, and Saxena, Rev. Mod. Phys. **20**, 334 (1948).

those which have begun to ionize heavily is uniform in range, i.e.,

$$F(R)dR = WdR, \quad (W = \text{constant}). \qquad (13)$$

The resulting calculated curves, fitted as regards frequency to the experimental curves, are labeled "positive excess protons" in Fig. 15. The fit appears to be less staisfactory than would be obtainable with a modified Bagge distribution because the smaller bursts in this case are produced mainly by protons of high energy and are not of sufficiently different size in nitrogen and argon. Nevertheless, protons of higher energy than given by the Bagge distribution have been found at sea level by Shutt[44] in about adequate numbers. It is evident that speculations of this kind will not be conclusive until much more extensive and reliable experimental data has been obtained.‡

(c) *Alpha-Particles*

Referring again to Fig. 13 and the component labeled "fragmentation alphas," if it is assumed that these emerge from the aluminum wall with a Bagge distribution, the rate of occurrence is five times less (3.0×10^{-3}/sq. cm/day) than that found for steel in the large ion chamber. But in the case of the small ion chamber, alpha-particles and protons from stars originating in the gas must also be important (unless stars tend to occur preferentially in dense matter). Failure to resolve this discrepancy underlines the need for better experimental data.

Run *L* with nitrogen was not of sufficient dura-

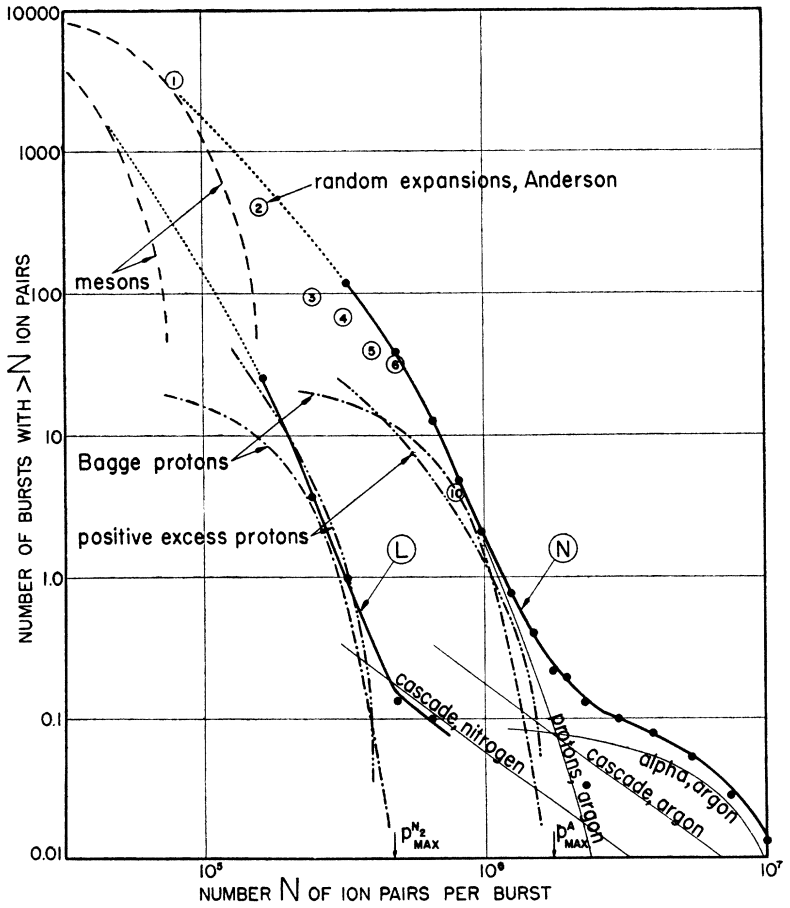

FIG. 15. Calculated bursts caused by single mesons and by single protons compared with the bursts observed in nitrogen and in argon in the small ion chamber; also the cloud-chamber showers of Anderson (see reference 45) (random expansions).

[44] P. R. Shutt, Phys. Rev. 69, 261, 272 (1946).

‡ Experimenters are recommended to use for this work ion chambers of spherical shape because a large fraction of the paths in a sphere are nearly equal in length to the maximum path length.

tion to establish the less steep branch accurately, but the data that was obtained is not inconsistent with the assumption that the less steep branch in nitrogen consists chiefly of cascades, as indicated in Fig. 15. It follows that the "alpha"-component has been considerably suppressed by recombination in nitrogen (see Table VII), which is consistent with the conjecture that it is probably produced by protons and alpha-particles of short range.

(*d*) *Showers*

It must be emphasized that the above analysis of these measurements is highly speculative and that bursts due to other effects are certainly superposed. For example, in Fig. 15 the early data of Anderson[45] on the relative numbers of single, double, etc., tracks found in random cloud-chamber expansions are plotted in comparison with the argon curve *N*. This data indicates that small showers are present which are very much more frequent than the extensive air cascades. This comparison was the basis of our previous opinion,[4] that the steep branches were composed entirely of showers and the numbers of particles in the showers, given within the circled points in Fig. 15, are the same as previously estimated.[4] It will be noted that the data now include showers of only 4 rays. Clay[46] thinks that the extensive showers have pronounced local concentrations of rays. Euler[6] also (Fig. 8, curve *W''*) has provided a steep branch of cascade showers resulting from fluctuations of density in the air cascades.

Finally, the component in Fig. 13 which has been provisionally labeled "protons, lead" must be discussed. It seems probable that this component is composed mainly of cascade showers. The evidence for this comes from the air-lead transition curve for bursts larger than 10^6 ion pairs measured by Chou (see Fig. 3 of the adjoining paper). This curve is a typical Rossi transition curve with maximum at 2 cm of lead. It should therefore probably be concluded for the present that most of the difference between "protons, unshielded" and "protons, lead" is due to small cascades from the lead, and these then may be added to the "cascades, lead" component to give a resultant curve very similar in shape to the curve *WW''* of Euler in Fig. 8.

6. ACKNOWLEDGMENTS

The experimental recordings discussed in this paper were obtained at the Cavendish Laboratory, Cambridge, under the supervision of Lord Rutherford.

Remeasurement of the records and study of the results was carried out at the Chalk River Laboratory of the National Research Council of Canada on a part-time basis. The writer's thanks are due the National Research Council of Canada for a liberal policy which enabled this to be done.

As already mentioned in footnotes, considerable assistance was obtained from members of the Theoretical Branch of the Laboratory directed by Dr. W. H. Watson.

Publication of the work of C. N. Chou[47] (preceding paper), now at the National Central University, Nanking, China, has taken an unduly long time. The writer regrets the delay.

[45] Andreson, Millikan, Neddermeyer, and Pickering, Phys. Rev. **45**, 352 (1934).
[46] J. Clay, Physica **11**, 311 (1945).
[47] Collected Papers, College of Science and Engineering, National University of Amoy, China **1**, 1 (1943).